

A CFD STUDY OF HYPERSONIC WEAKLY-IONIZED ARGON PLASMA FLOW

Tarit K. Bose^s

Metacomp Technologies, Inc., Westlake Village, CA 91361

Abstract

A multiple-specie argon plasma flow with weak ionization at hypersonic speeds for the heavy particles is studied with a single-step time-dependent method. The charge separation that may occur behind the shock is based on the premises that while the heavy particle flow is supersonic, the electron flow is subsonic. Therefore, the charge separation should induce a strong electric field and several approaches are discussed to compute such electric field in the flow or opposite flow direction of the atoms and ions. Finally an approach is considered, where the electric field is computed from the pressure gradient of electrons only, which is the equilibrium condition for the electron momentum equation of a stationary plasma. Separate continuity and momentum equations are written for electrons, ions and neutrals, and separate energy equations are written for the heavies and the electrons. Change in the shock structure and reduction in the drag coefficient are demonstrated for argon plasma.

Nomenclature

b	= mobility coefficient, $m^2/V/s$
c_1-c_3	= constants controlling various terms
c_D	= drag coefficient
E	= electric field, V/m
e	= elemental charge = 1.602×10^{-19} As
e_j	= internal energy of j -th specie, J/kg
F	= volumetric force, N/m^3
g	= relative kinetic speed, m/s
h	= specific enthalpy, J/kg
I	= ionization potential (energy), J
j	= electric current density, A/m^2
k_B	= Boltzmann constant = 1.38×10^{-23} J/K
M	= mass of a single particle, kg
m	= mole mass, $kg/kmol$
n	= number density of the particles, m^{-3}
n_c	= charge density, As/m^3
p	= pressure, N/m^2 or bar
Q	= collision cross-section, m^2
R^*	= universal gas constant = 8314 J/kmol/K
r	= radial coordinate
T	= temperature, K
V	= velocity vector, m/s
V^*	= mean velocity of flow, m/s
V_f	= field velocity, m/s
u_∞	= approaching flow velocity, m/s
v	= kinetic speed, m/s
x	= mole fraction
ϵ_0	= dielectric constant (in vacuum) = 8.855×10^{-12} As/V/m
ϕ	= electric potential, V
Γ'	= volumetric collision frequency, $m^{-3}s^{-1}$
λ_D	= Debye shielding distance, m
λ	= mean free-path
θ	= azimuthal coordinate
θ	= temperature ratio T_0/T_h
ρ	= mass density, kg/m^3

Subscripts and superscripts

a	= atom
b	= body
d	= diffusion
e	= electron
h	= heavies
i	= ion
j	= a specie
(\cdot) *	= non-dimensional quantity
∞	= approaching flow state

Introduction

⁵Senior Scientist. Associate Fellow, AIAA.
Copyright © 2001 by Metacomp Technologies, Inc.
Published by the American Institute of Aeronautics and
Astronautics, Inc., with permission.

Russian experiments with weakly ionized gases at supersonic speeds have been reported for many years¹⁻¹¹, but only in recent years there is great interest in the subject elsewhere also¹². These experiments were conducted with Ar, Kr, Xe, CO₂, N₂, CF₂Cl₂, CF₄ and air, where the weakly ionized plasma was generated through a number of methods like pulse discharge, glow discharge, microwave pulse and pulsed laser. Typical plasma states obtained were: electron temperature 1 to 4 eV (equivalent of 11,600 to 46,400 K), heavy particles (gas) temperature 500 to 1,500 K, pressure 10 to 70 Torr, degree of ionization 10⁻⁶ to 10⁻⁵. Thus we are concerned with plasmas, which are, both thermally and chemically, at highly non-equilibrium states. For such weakly ionized plasmas some of the features of a ballistic model, flying at supersonic speeds but after entering the local regions of weakly ionized air, include: (a) the shock stand-off distance increases several times, (b) there is an apparent decrease in the Mach number and density, and (c) reduction in the drag coefficient. While the above features are dominant when the flowing medium is air, these features are present also to a lesser extent if a noble gas like argon is taken. If it is presumed that in air there may be considerable dissociation and ionization due to electrons at a strongly elevated temperature¹³, which may at least be responsible partly for these features, then it is quite in order for an initial study to have a noble gas like argon as a flowing medium. This is the main motivation for the present study and thus the objective of the present study is to develop a workable procedure to compute hypersonic flow of a weakly ionized plasma over a blunted body, which should explain experimental results for such gases.

For the effects in weakly ionized plasmas, it is mentioned in Ref. 14, that in the vicinity of a shock the ions slow down and their number density increases. Matching of electron and ion number density requires that the electrons be trapped in the downstream side. It is, however, not evident how the above description for a one-dimensional case may get translated into the two- or three-dimensional case, for example for a hypersonic flow over a blunted inverted cone which is the present case.

For plasma flows there can be several different approaches to determine the electric field. Firstly, it can be determined from the externally imposed voltage, which is not the case here. Secondly, in situations in which charge neutrality does not hold, Poisson equation may be used. Thirdly, without any externally applied electric field it can be determined from the ambi-polar type of analysis; and fourthly, some authors^{15,16} have suggested, that one could compute electric field from the electron pressure gradient, which is derived from the electron

momentum equation by dropping all convective terms (equilibrium case).

For the wall boundary condition, initially both the fully electrical conducting and non-conducting walls were considered, but the difference in flow and electric fields were found to be only in the immediate vicinity of the body. However for an electrically non-conducting wall the local electrical potential is obtained from the flow field and no other boundary conditions on electric potential or electric field need be followed strictly. Therefore, in the present study only the electrically non-conducting wall was considered.

Highlight of the present analysis is that we consider three specie non-equilibrium (both thermal and chemical) gas plasma without considering quasi-neutrality. Separate equations of mass and momentum for neutrals, electrons and ions, and separate energy equations for heavy particles and electrons are used. Estimates of reaction rates for ionization and recombination for a highly non-equilibrium weakly ionized plasma are not known and hence the "frozen chemistry" was considered. Any change in the number density of the charged particles will, therefore, only be due to the pressure field and the collision and electric field forces acting on the particles. Similarly since the energy exchange mechanism due to collision for a non-equilibrium plasma like a weakly ionized plasma is not known well, the term representing the energy exchange between the heavies and the electrons is put equal to zero at this time.

CFD field calculations are done with Lax-Friedrich method with separate CFL numbers and time steps for heavies and electrons. Obviously, the electron sonic speed is much larger than that of heavies, and the electron time-cycle is embedded into the heavies time-cycle. For geometry a blunted reverse cone in hypersonic flow is considered (Fig. 1), which, for an ideal gas, was studied by Bohachevsky and Mates¹⁷ using the same numerical method.

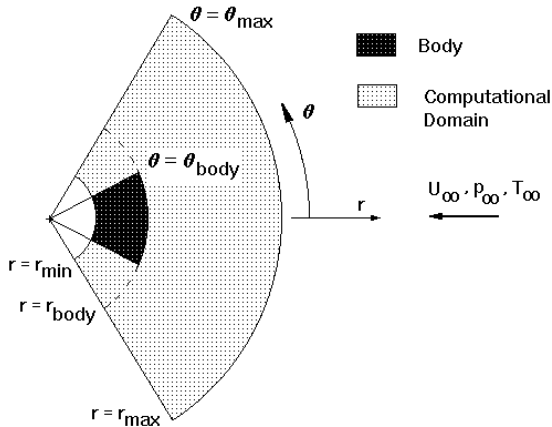


Fig. 1 Model of a Blunted Reverse Cone in Hypersonic Flow

Analysis

Electric Field Models

As mentioned already in the Introduction several electric field models were considered. These are now discussed briefly.

(a) *Poisson equation:*

We write now the one-dimensional Poisson equation, but the right hand source term with the opposite sign. This can be explained by the fact, that since there is no externally applied electric field, if it is computed for charge distribution behind the shock with the help of Poisson equation with the usual sign convention, then this latter electric field will be just exact and opposite of the former, which is then the induced electric field and potential. Thus we write

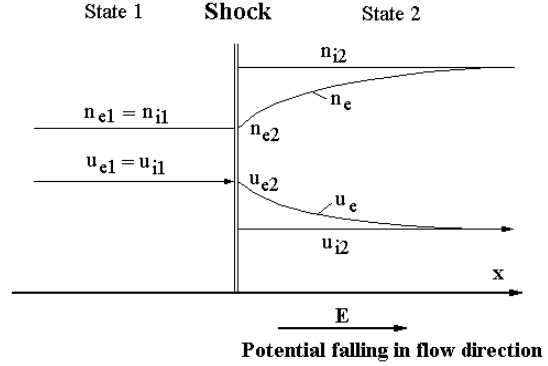


Fig. 2 Schematic sketch of distribution of number density and flow speed of ions and electrons across a 1-D shock and the electric field behind the shock.

$$\frac{d^2\phi}{dx^2} = \frac{e}{\epsilon_0} (n_i - n_e) = \frac{en_{i2}}{\epsilon_0} \left[\frac{n_i}{n_{i2}} - \frac{n_e}{n_{i2}} \right]$$

(1)

where subscript "2" refers to the state just after the shock (Fig. 2). Note that the electron temperature and electron number density do not change right across the shock and any change in these are only downstream of the shock. We introduce the following non-dimensional variables:

$$n_i^* = \frac{n_i}{n_{i2}}, n_e^* = \frac{n_e}{n_{i2}}, \phi^* = \frac{e\phi}{k_B T_{e2}}, x^* = \frac{x}{\lambda_D}, n_2^* = \frac{n_{e2}}{n_{i2}}$$

where

$$\lambda_D = \sqrt{\frac{\epsilon_0 k_B T_{e2}}{e^2 n_{i2}}} = 69 \sqrt{\frac{T_{e2}}{n_{i2}}} \quad [\text{m}]$$

(1a)

The expression in Eq. (1a) is the relation for the Debye shielding distance, but in a modified form, in which the electron number density is replaced by ion number density [m⁻³]. Obviously for large electron temperature and small ion number density the Debye shielding

distance in the present case is quite large and may be responsible for some of the effects in a weakly ionized plasma. We obtain now the Poisson equation in non-dimensional form as

$$\frac{d^2 \phi^*}{dx^{*2}} = 1 - n_e^* \quad (1b)$$

From the boundary conditions $x^* = 0 : n_e^* = n_2^*$, $x^* \rightarrow \infty : n_e^* = 1$ (Fig. 2), and we select a trial solution

$$n_e^* = 1 + (n_2^* - 1) \exp^{-x^*}$$

and we get the following expressions for potential and electric field in dimensional form as

$$\phi = \frac{k_B T_e 2}{e} \left(-n_2^* \right) \exp^{-x/\lambda_D} \quad (2)$$

$$\mathbf{E} = \frac{k_B T_e 2}{e \lambda_D} \left(-n_2^* \right) \exp^{-x/\lambda_D} \quad (3a)$$

We see from the expressions that the electric field is in the flow direction and the potential is also falling in the flow direction, thus satisfying both the requirements. However, this model is difficult to apply for multi-dimensional case.

(b) Diffusive model:

We consider now, at least conceptually, similarity with "ambi-polar diffusion model" for a quasi-neutral plasma. Basic idea here is that there are separate gasdynamic sonic speeds for heavies and the electrons. While for the heavy particles the flow is supersonic and there can be gas dynamic shock, the electrons, because of their very small mass and consequently very large sonic speed, remain subsonic in the entire flow domain and are largely unaffected. Thereby we assume an electric field, \mathbf{E} , which is required for the restoration of the condition of equal flux of the electrons and the ions.

Now we first define an average velocity of the particles as

$$\mathbf{V}^* = \frac{n_a \mathbf{V}_a + n_e \mathbf{V}_e + n_i \mathbf{V}_i}{n_e + n_i + n_a} \approx \mathbf{V}_a$$

The current density for electrons and ions are given by the relations

$$\begin{aligned} \mathbf{j}_e &= -en_e(\mathbf{V}_e - \mathbf{V}^*) + en_e |b_e| \mathbf{E} \\ \mathbf{j}_i &= en_i(\mathbf{V}_i - \mathbf{V}^*) + en_i |b_i| \mathbf{E} \end{aligned}$$

Further for modeling of an equivalent of ambi-polar diffusion type, $\mathbf{j}_i = -\mathbf{j}_e$, which gives us finally the equation for the electric field

$$\begin{aligned} \mathbf{E} &= \frac{\mathbf{V}^*(n_i - n_e) - (n_i \mathbf{V}_i - n_e \mathbf{V}_e)}{n_i |b_i| + n_e |b_e|} \\ &= \frac{n_e \mathbf{V}^* - e(n_i \mathbf{V}_i - n_e \mathbf{V}_e)}{e(n_i |b_i| + n_e |b_e|)} \end{aligned} \quad (3b)$$

Herein n_i, n_e are number density of ions and electrons given in $[m^{-3}]$, n_e is the charge density in $[As/m^3]$, $\mathbf{V}_i, \mathbf{V}_e$ are velocity of ions and electrons in $[m/s]$, b_i, b_e are the respective mobility coefficients, and \mathbf{E} is the required electric field in $[V/m]$. Since across a shock the flux of electrons and ions separately do not change and because of equal electron and ion flux at the approaching flow boundary (quasi-neutrality condition), the second term in the numerator of the above equation should be negligible. The electric field is again in the direction of the velocity field of the neutrals.

(c) Equilibrium model:

This uses a simplified equilibrium form of the electron momentum equation by neglecting all terms other than the pressure gradient and electric field terms to get the relation for electric field proportional to the negative of the electron pressure gradient^{15,16}

$$\mathbf{E} = -\frac{1}{en_e} \nabla p_e \quad (3c)$$

As mentioned already, our first conjecture regarding the electric field was, that there will be positive charge density behind the shock, causing an electric field in the flow direction to affect further the flow properties. An important consideration in such a model is, of course, that the electrons and ions will not recombine and vanish behind a shock, the number density of neutrals and ions increase substantially behind the shock with consequent reduction in their flow speeds, whereas for the electrons there may not be much change either in the flow velocity or the number density. However, further downstream of the shock the electrons need to be decelerated with the consequent increase in the number density of the electrons, while the ion flow speed may increase and ion number density may decrease in the flow direction. However, in actual calculations it was found that the ions are pushed in the flow direction and the electrons in the opposite direction. Since, for the electrons the flow is subsonic, the electrons are forced to move all the way to the approaching flow boundary of the charged particles and the heavies are pushed more towards the wall. This causes very large negative potential at the wall with respect to the approaching flow boundary and also it becomes difficult to obtain convergence in a steady flow solution. On the other hand, the

equilibrium model gives the electric field away from the body and a fairly stable solution.

After computing the electric field everywhere, it is now possible to get the electric potential by integrating the electric field in all coordinate directions after starting from the value of the potential at a specified location, which has been put as zero at the approaching flow boundary.

Body Geometry

The body being considered is that of an inverted cone with a spherical shaped front surface (shown black in Fig. 1)(Bohachevsky and Mates¹⁷). The grey area in the same figure is the computational domain. As in Ref. 17, the flow equations are written in spherical (r, θ, χ) coordinates, in order to calibrate the present method with those for ideal non-ionized gas (Bohachevsky and Mates or B&M method). Subsequently the equations are written for the axi-symmetric case by putting equal to zero the velocity component in χ direction and all derivatives with respect to χ . After the solution reaches a steady state, aerodynamic drag (and thermal loading, if necessary) can be computed easily by integrating over the surface. In order to understand the process both the electrically conducting and non-conducting wall have been considered but finally only electrically non-conducting wall is discussed here.

Basic Equations

We consider here a singly-charged weakly ionized plasma with electron and ion mole fraction, x_e and x_i , respectively, pressure p , the heavy particles translational temperature T_h and the electron temperature T_e . Obviously the mole fraction of the atom is

$$x_a = 1 - (x_e + x_i)$$

Equation of state ($\theta = T_e/T_h$) can now be written as

$$p = nk_B [x_e T_e + (1 - x_e) T_h] = \frac{nk_B T_e}{\theta} [1 + (\theta - 1)x_e] \quad (4)$$

and for a given pressure, two temperatures and electron mole fraction, it is easy to compute the total number density. Further, by knowing the mole fraction of either ion or atom, it is possible to compute the number densities of all the three, which is the method to determine these at the incoming boundary.

For each of the j -th specie ($j = a, i$ or e) and without any reaction, the continuity equation can now be written as

$$\frac{\partial \rho_j}{\partial t} + \nabla \cdot (\rho_j \mathbf{V}_j) = 0 \quad (5)$$

The right hand side of the equation is zero, since we consider "frozen chemistry" in the plasma. Further the

general expression for the momentum equation (for inviscid case) for the j -th specie is written as

$$\frac{\partial}{\partial t} (\rho_j V_j^r) + \nabla \cdot (\rho_j V_j^r \mathbf{V}) = -\nabla p_j + F_j^r$$

(6)

where M_j is the mass of a particle of the j -th specie and Γ'_{jk} is the volumetric collision frequency [$\text{m}^{-3}\text{s}^{-1}$] between j -th and k -th species. The volumetric force term in the r -th direction is given by the relation

$$F_j^r = c_1 n_j e_j E^r + c_2 \sum_{j \neq k} \frac{2M_j M_k}{(M_j + M_k)} (V_k^r - V_j^r) \Gamma'_{jk}$$

(6a)

where c_1 and c_2 , with values between 0 and 1, are two coefficients used for controlling the effect of these terms. The first term in the right hand side of Eq. (6a) is the volumetric force term due to electric field on the charged particles and the second is the velocity equilibration term due to collision.

The electric field term is supposed to act continuously on charged particles causing it to accelerate. However, it is well known that in a collision dominated plasma the acceleration can not go on continuously and till the maximum directional particle velocity in the field, so

called field velocity, $\mathbf{V}_f = b_j \mathbf{E}$ is reached (b_j is the so-called "mobility coefficient"). Since the induced electric field (in absence of an externally applied electric field) and the number density are directly proportional to the pressure and the volumetric collision frequency is proportional to the square of the pressure, the mobility coefficient is inversely proportional to the pressure. Therefore, both the terms for volumetric force as given in Eq. (6a) are directly proportional to the square of the pressure. Obviously a very large value of source terms in partial differential equations make them very stiff and unless special provisions are made for handling the equations the solution may blow up at high level of pressure field. This is done by writing the source terms in implicit manner.

Further the specific stagnation enthalpy and the stagnation internal energy (per unit mass) of individual species are given by the relations

$$h_j = \frac{R^*}{m_j} \left[\frac{5T_j}{2} + \frac{I_j}{k_B} \right]; e_j = \frac{R^*}{m_j} \left[\frac{3T_j}{2} + \frac{I_j}{k_B} \right]$$

(7a,b)

where $R^* = 8314$. J/(kmole.K) is the universal gas constant, I_j is the ionization potential and m_j is the

mole mass of the j -th specie. It is obvious that $I_a = I_e = 0$.

The heavy particles and electrons energy equations are:

$$\begin{aligned} \frac{\partial}{\partial t}(\rho_a e_a + \rho_i e_i) + \nabla \cdot (\rho_a h_a \mathbf{V}_a + \rho_i h_i \mathbf{V}_i) &= en_i b_i E^2 \\ + 3c_3 \sum_{k=a,i} \frac{m_e}{m_k} k_B (T_e - T_h) \Gamma'_{ek} + \sum_{k=a,i} (\mathbf{V}_k \nabla) \cdot p_k \\ \frac{\partial}{\partial t}(\rho_e e_e^o) + \nabla \cdot (\rho_e h_e^o \mathbf{V}_e) &= en_e b_e E^2 \\ - 3c_3 \sum_{k=a,i} \frac{m_e}{m_k} k_B (T_e - T_h) \Gamma'_{ek} + (\mathbf{V}_e \nabla) \cdot p_e \end{aligned} \quad (8a,b)$$

where c_3 is again a source control coefficient for the two energy equations, b 's are the mobility coefficients and \mathbf{E} is the externally applied electric field. Since we are not considering any externally applied electric field, the first term in the right hand side of Eqs. (8a,b) have been put equal to zero. Further, we studied the case of $c_3 = 1$ (electron-ion energy exchange term considered) and it was found that the electron temperature drops drastically right after the approaching flow boundary. Therefore, further study with $c_3 = 0$ is done in this paper.

Values of the volumetric collision frequency and mobility coefficient required in our calculations are obtained by calculating first the collision cross-section, etc. The method to obtain these are given in Ref. 18.

We would now like to discuss the boundary conditions. For non-conducting wall, the normal component of the velocity of both electrons and heavies are zero, whereas for conducting wall, only the normal velocity component of heavies is zero. The boundary conditions on the approaching flow boundary are prescribed, whereas the boundary conditions in exit boundaries are obtained by extrapolation. Wall boundary condition for the heavies is always no-slip condition for the temperature and the normal velocity components are zero.

Drag coefficient

The drag coefficient for the present body (Fig. 1) is given by the relation

$$c_D = \frac{2}{\rho_\infty u_\infty^2 \sin^2 \theta_b} \int_0^{\theta_b} (p - p_\infty) \sin(2\theta) d\theta$$

In the hypersonic approximation, Newton's law gives

$$(p - p_\infty) = \rho_\infty u_\infty^2 \cos^2 \theta$$

and the drag coefficient in the hypersonic limit is

$$c_D = 1 + \cos^2 \theta_b \quad (9)$$

Incidentally for a flat plate perpendicular to the flow direction in the hypersonic limit ($M_\infty \rightarrow \infty$), $\theta_b \rightarrow 0$; $c_D = 2$ and for a monatomic gas like argon the stagnation point density to free-stream density ratio is 4.0. In addition for the present case with $\theta_b = 32^\circ$, c_D in the hypersonic limit is 1.7192.

Grid Independence

In order to test the grid independence of the numerical results, calculations were done for neutral argon as an ideal gas for three different grids. The overall data considered were the stagnation point pressure and density, and the drag coefficient. Comparative results for unionized argon are given in Table 1, along with results obtained theoretically from the Hypersonic Theory and for the weakly ionized argon. While the density in the stagnation region in the hypersonic limit is 0.0137 kg/m^3 , for $M_\infty = 6.02$ the pressure and density in stagnation region is 0.4505 bar and 0.0127 kg/m^3 , respectively.

In addition, the density distribution on axis for the three grids are shown in Fig. 3. An important result, originally shown by Bohachevsky and Mates¹⁷, showed that the maximum density is obtained right after the shock and then it falls in the stagnation region behind the shock due to very strong flow acceleration in the lateral direction. If we consider the distance from the wall stagnation point to the point of maximum density value on the axis as the shock stand-off distance, this can be compared easily with the experimental data summarized by Liepmann and Roshko¹⁹ for a sphere in hypersonic flow of Mach 6. These comparisons show that the grid size (145x19) is good enough for the present calculations.

Table 1. Drag coefficient, and stagnation point density and pressure for neutral argon

Calcul. method	grid	c_D	p_{stag} [bar]	ρ_{stag} [kg/m ³]
B&M ($M_\infty = 6$)	73x11	2.351	0.8398	0.0128
	145x19	1.673	0.6208	0.0118
	289x37	1.429	0.5687	0.0113
Theor. ($M_\infty \rightarrow \infty$)		1.719	∞	0.0137
Theor. ($M_\infty = 6$)			0.4505	0.0127

B&M Ar- plasma	145x19	1.098	0.3817	0.0154
----------------------	--------	-------	--------	--------

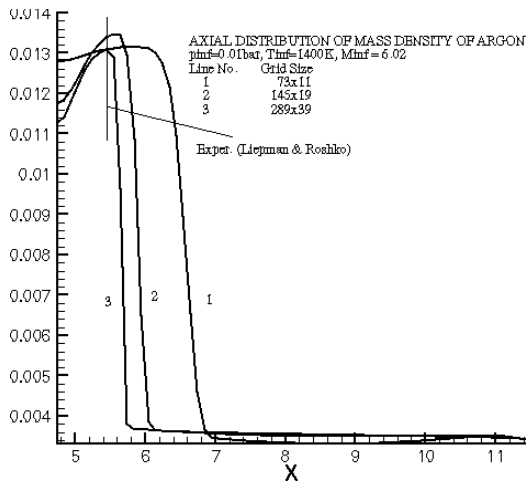
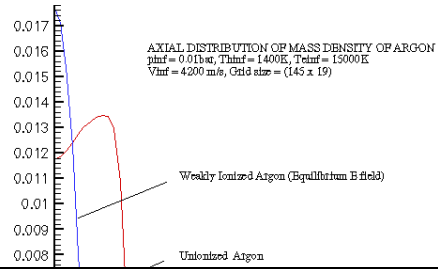


Fig. 3 Comparison of mass–density distribution on axis for unionized argon for different grids

Numerical Procedure

For our computation a typical weakly ionized argon plasma ($p_\infty = 0.01$ bar, $V_\infty = 4,200$ m/s, $T_{e\infty} = 15,000$ K, $T_{h\infty} = 1,400$ K and $x_{e\infty} = 10^{-6}$) is considered and comparison is made with fully neutral argon gas with equivalent Mach number of 6.02. It was found that, because of their very small mass, the electron flow and field variables can change very strongly and a CFL value of 0.2 for electrons was the maximum that was used in order to get a stable solution while the CFL value for heavies was about 0.7. Because of very large difference in time scales between heavies and electrons, typically 50 to 80 time steps for electrons was taken inside each time step of the heavies. A total of 250 to 300 time–steps (including about 100 steps at the largest CFL numbers) was found to get an adequate convergence. During our calculations initially $c_D = 0$, but it increases first with increasing time steps, reaches a maximum and flattens out or decreases slightly; a change of c_D value less than 0.0005 per time step with CFL value for heavies about 0.7 are considered adequate to stop further calculations. The numerical method used here is the Lax–Friedrich single–step time–dependent method, which follows closely the method and application of boundary conditions used by Bohachevsky and Mates¹⁷, except that here we have computed with multiple species at multiple temperatures and in electric field developed due to charge separation. Separate time scales are used for electrons and heavy particles. Typically, electron time scale is about one–sixtieth of that of heavies and change considerably from the approaching to exit boundary.



Gas	grid	c_D	P_{stag} [bar]	ρ_{stag} [kg/m ³]
Neutral argon	73x11	2.351	0.839	0.012
			8	8
	145x19	1.673	0.620	0.011
			8	8
Argon plasma (Equil.)	289x37	1.429	0.568	0.011
			7	3
	145x19	1.098	0.381	0.015
			7	4

body, the weakly ionized argon result shows that there is considerable increase in the density before the body. In addition, while, for unionized gas there is maximum density away from the wall (shock–standoff distance), this was not observed for the weakly ionized argon.

Further if the point of sharp increase of atom mass density can be considered as the shock–standoff distance, the plot of mass–density contour for unionized argon in Fig. 5 and for argon plasma in Fig. 6 show that the shock–standoff distance actually reduces slightly for the latter case. The results for weakly ionized argon appear to be opposite the experimental evidence where for plasma it is almost the size of the one for the gas²⁰.

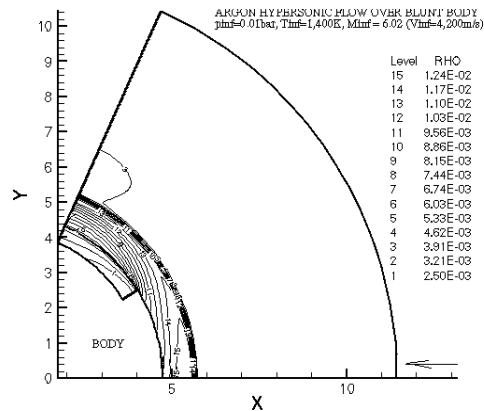


Fig. 5 Contour Plot of Mass–density of Unionized Argon

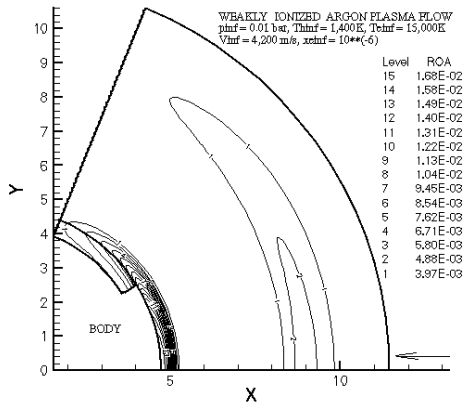


Fig. 6 Contour Plot of Mass-density of Atoms in a Weakly Ionized Argon Plasma

Since, in present calculations the energy exchange term in energy equations for heavies and electrons have been deactivated, any increase in the temperature of these are due to compression in front of the body and any decrease is due to expansion around the corner of the body. This is shown with the help of the contour plot for electron temperature in Fig. 7 and for heavies temperature in Fig. 8. While for the former the ratio of maximum temperature to approaching flow temperature is about 1.3, for the latter the ratio is almost 6.7.

Finally, we discuss the electric field and potential distribution for the weakly ionized plasma. The results are exclusively for the equilibrium electric field model, where the electric field, due to increase in partial pressure of electrons in the stagnation region, is against the flow direction. On the other hand in the expansion region around the corner of the body the electric field is in the direction of the flow. Therefore in front of the body due to "stagnation effect", the electrons are "pushed" towards the body, but the ions are pushed away from the body. The resulting electric field develops in the entire region of weakly ionized flow all the way till the approaching flow boundary and there is a very strong electric field right at the boundary (Fig. 9). Further Fig. 10 shows the electric potential distribution on the axis, and Fig. 11 shows the contour plot of the electric potential.

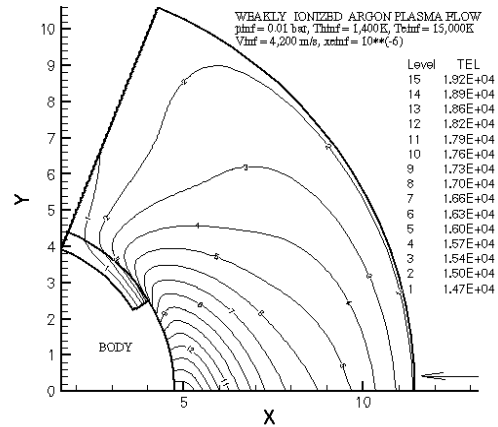


Fig. 7 Contour Plot of Electron Temperature in a Weakly Ionized Argon Plasma

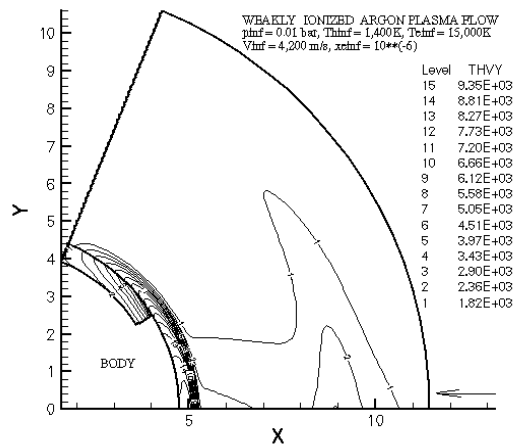


Fig. 8 Contour Plot of Temperature of Heavies in a Weakly Ionized Argon Plasma

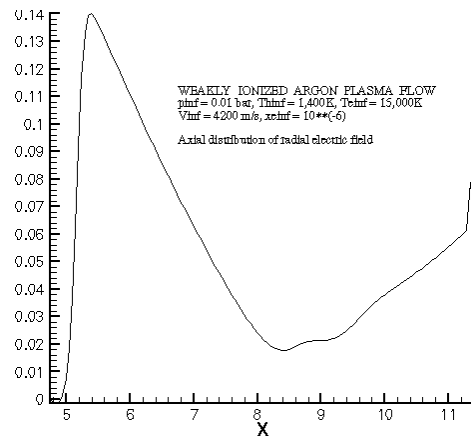


Fig. 9 Radial Electric Field on Body Axis

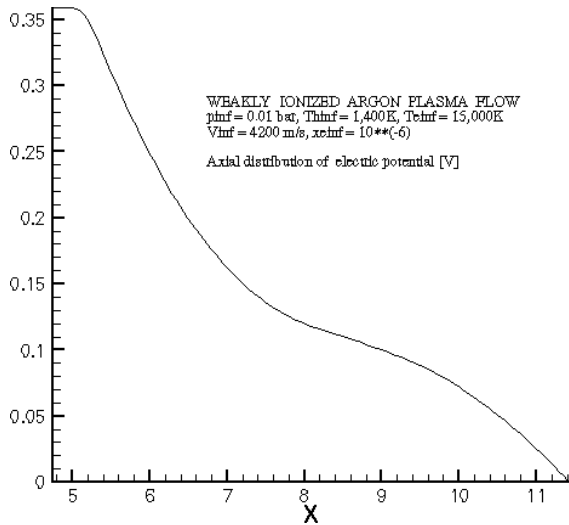


Fig. 10 Radial Electric Field on Axis for a Weakly Ionized Argon (Non-conducting Wall)

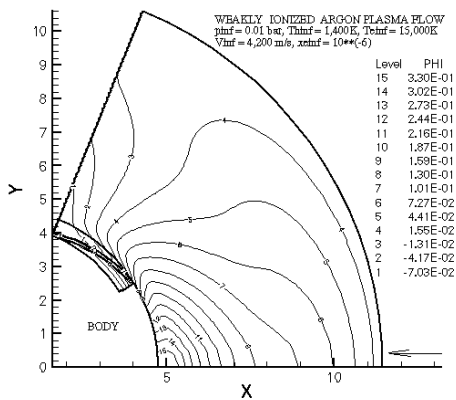


Fig. 11 Contour Plot of Electric Potential for a Weakly Ionized Argon (Non-conducting Wall)

Summary and Conclusions

On the basis of numerical experimentation we can make the following conclusions:

1. With separate equations for electrons, ions and neutrals we can compute weakly ionized flow and obtain the characteristic results, like smaller drag coefficient and splitting of the shock in a large domain, in comparison to the shock in a unionized gas;
2. One has to consider separate time steps for heavies and electrons; as such, the electrons behave as if there is a subsonic flow, although the heavies flow speed is supersonic. As a result charge separation takes place creating local electric field in the entire flow domain with weakly ionized plasma to affect the velocity field of all particles; and

3. A very drastic change of the shock shape in weakly ionized argon plasma was not seen, which compares well with the results in Ref. 20. It may, however, be necessary to extend the present approach to a dissociative gas or gas mixture like air.

References

1. G.I. Mishin, A.P. Bedin and I.P. Yavor, "Properties of Gas Behind a Shock Wave During Anomalous Relaxation", *Soviet Technical Physics Letters*, Vol. 8, No. 2, Feb. 1982, pp. 79–80.
2. G.I. Mishin, "Shock Waves in a Weakly Ionized Non-isothermal Plasma", *Soviet Technical Physics Letters*, Vol. 11, No. 3, March 1985, pp. 112–14.
3. L.P. Grachev, I.I. Esakov, G.I. Mishin, M. Yu. Nikitin, K.V. Khodataev, "Interaction of a Shockwave with a Decaying Plasma in an Electrodeless Microwave Discharge", *Soviet Physics Technical Physics*, Vol. 30, No. 5, May 1985, pp. 586–88.
4. A.F. Alexandrov, N.G. Vidyakin, V.A. Lakutin, M.G. Skvortsov, I.B. Timifeev, V.A. Chenikov, "A Possible Mechanism for Interaction of a Shockwave with a Decaying Laser Plasma", *Soviet Physics Technical Physics*, Vol. 31, No. 4, April 1986, pp. 468–69.
5. V.P. Goloviznin, G.I. Mishin, Yu.L. Serov and I.P. Yavor, "Supersonic Flow Around a Sphere in a Thermal Irregularity", *Soviet Physics Technical Physics*, Vol. 32, No. 7, July 1987, pp. 853–55.
6. V.A. Gorshkov, A.I. Klimov, G.I. Mishin, A.B. Fedatov and I.P. Yavor, "Behaviour of Electron Density in a Weakly Ionized Non-equilibrium Plasma with a Propagating Shock Wave", *Soviet Physics Technical Physics*, Vol. 32, No. 10, Oct. 1987, pp. 1138–41.
7. A.I. Klimov, G.I. Mishin, "Interferometric Studies of Shock Waves in a Gas Discharge Plasma with a Propagating Shock Wave", *Soviet Technical Physics Letters*, Vol. 16, No. 12, Dec. 1990, pp. 960–62.
8. G.I. Mishin, Yu.L. Serov and I.P. Yavor, "Flow Around a Sphere Moving Supersonically in a Gas Discharge Plasma", *Soviet Technical Physics Letters*, Vol. 17, No. 6, June 1991, pp. 413–16.
9. G.I. Mishin, "Total Pressure Behind a Shock Wave in Weakly Ionized Air", *Technical Physics Letters*, Vol. 20, No. 11, Nov. 1994, pp. 857–59.
10. A.P. Bedin and G.I. Mishin, "Ballistic Studies of the Aerodynamic Drag on a Sphere in Ionized Air", *Technical Physics Letters*, Vol. 21, No. 1, Jan. 1995, pp. 5–7.
11. V.P. Gordeev, A.V. Krasilnikov, V.I. Lagutin and V.N. Otmennikov, "Experimental Study of the Possibility of Reducing Supersonic Drag by

- Employing Plasma Technology", *Fluid Dynamics*, Vol. 31, No. 2, 1996, pp. 313–17.
12. L. Bain, "Overview of Research into Aerodynamic Behaviour in Weakly Ionized Gases", *Oral Invited Presentation*, 37th Aerospace Sciences Meeting and Exhibit, Reno/NV, Jan. 11–14, 1999.
 13. C. Park, R.L. Jaffe and H. Partridge, "Chemical Kinetic Parameters of Hyperbolic Earth Entry", *AIAA Paper 00–0210*, 38th Aerospace Sciences Meeting and Exhibit, Reno/NV, Jan. 10–13, 2000.
 14. H.W. Friedmann, L.M. Linson, R.M. Patrick and H.J.E. Petschek, "Collisionless Shocks in Plasmas" in *Annual Reviews of Fluid Mechanics*, Vol. 3, 1971, pp. 63–33.
 15. G.V. Candler and R.W. MacCormack, "'Computation of Weakly Ionized Hypersonic Flows in Thermochemical Nonequilibrium", *J. Thermophysics and Heat Transfer*, Vol. 5, No. 3, July–Sept. 1991, pp. 266–73.
 16. S. Qarnain and M. Martinez–Sanchez, "Issues Regarding the Generation of an End–to–End Hall Transfer Computational Model", *AIAA Paper 98–3796*, 34th AIAA/ASME/SAE/ASEE Joint Propulsion Conference, July 13–15, 1998, Cleveland, OH.
 17. I.O. Bohachevsky and R.E. Mates, "A Direct Method for Calculation of the Flow about an Axisymmetric Body at Angle of Attack", *AIAA Jl.*, Vol. 4, No. 5, 1966, pp. 776–782.
 18. T.K. Bose, "Thermophysical and Transport Properties of Multi–component Gas Plasmas at Multiple Temperatures", *Progress in Aerospace Sciences*, Vol. 25, 1973, pp. 1–42.
 19. H.W. Liepmann and A. Roshko, *Elements of Gasdynamics*, Wiley, 1957.
 20. H. Lowry, M. Smith, P. Sherrouse, J. Felderman, J. Drakes, M. Bauer, D. Pruitt and D. Keefer, "Ballistic Range Tests in Weakly Ionized Argon", *AIAA Paper 99–4822*, 3rd Weakly Ionized Gases Workshop, Norfolk/VA, Nov. 1–3, 1999.

